

# Polymer Templated Synthesis of AgCN and Ag Nanowires

Thomas D. Lazzara,<sup>†</sup> Gilles R. Bourret,<sup>†</sup> R. Bruce Lennox,\* and Theo G. M. van de Ven\*

Department of Chemistry and Centre for Self Assembled Chemical Structures, McGill University,  
801 Sherbrooke Street W, Montreal, Quebec, H3A 2K6 Canada

Received September 12, 2008. Revised Manuscript Received March 6, 2009

A template-based method for the fabrication of silver cyanide and polymer composite nanowires is described. Poly(styrene-*alt*-maleic anhydride) forms nanotubes in aqueous solution and acts as a template, guiding the growth of silver cyanide into long nanowires. The structures obtained can grow to several tens of micrometers in length and their diameter range from several to tens of nanometers. These AgCN nanowires can be reduced to metallic silver to form a high surface area Ag(0) nanowire array on a flexible nylon filter substrate.

## 1. Introduction

Fabrication of one-dimensional metallic nanostructures is an important activity within nanoscience. Their ability to absorb and scatter light has led to numerous studies in plasmonics,<sup>1–9</sup> spectroscopy,<sup>8–12</sup> and biosensing.<sup>13–16</sup>

The size-dependent electrical properties of nanostructures are particularly relevant to nanoscale electronics studies.<sup>17,18</sup> Some of these materials have demonstrated exceptional catalytic properties because of their high surface area.<sup>19–24</sup>

Among the variety of nanomaterials available, silver nanostructures are especially important in the development of nanotechnology devices: silver is a low-cost and highly conductive metal, well-known for the intense and tunable optical response of its nanostructures.<sup>4–8,11,25</sup> These charac-

teristics suggest that silver nanostructures can be significant candidates to use in nanotechnology applications.

A variety of wet chemical,<sup>25–32</sup> template-based<sup>33–37</sup> techniques and physical vapor-phase syntheses<sup>38</sup> have been developed to fabricate silver nanowires and nanosized composite materials. Templating processes are versatile but can have clear disadvantages such as the need to dissolve the template. Thermolysis techniques<sup>36</sup> prevent formation of bare metallic structures on flexible organic substrates, whereas direct synthesis usually involves complex methods.<sup>28,39</sup> There are reports on the preparation of Ag(0) nanowire bundles from self-organized Ag(I) complexes<sup>40,41</sup> (silver thiolate and silver oxalate), but neither offers the possibility

\* Corresponding authors. E-mail: theo.vandeven@mcgill.ca; bruce.lennox@mcgill.ca.

<sup>†</sup> These authors equally contributed to this work.

- (1) Burda, C.; Chen, X.; Narayanan, R.; El-Sayed, M. A. *Chem. Rev.* **2005**, *105*, 1025.
- (2) Brongersma, M. L.; Hartman, J. W.; Atwater, H. A. *Phys. Rev. B* **2000**, *62*, R16356.
- (3) Dickson, R. M.; Lyon, L. A. *J. Phys. Chem. B* **2000**, *104*, 6095.
- (4) Kelly, K. L.; Coronado, E.; Zhao, L. L.; Schatz, G. C. *J. Phys. Chem. B* **2003**, *107*, 668.
- (5) Link, S.; El-Sayed, M. A. *J. Phys. Chem. B* **1999**, *103*, 8410.
- (6) Kreibig, U.; Vollmer, M. *Materials Science*; Gonser, U., Panish, M. B., Osgood, R. M., Sakaki, H., Lotsch, H. K., Eds.; Springer-Verlag: New York, 1995.
- (7) Evanoff, D. D.; Chumanov, G. *ChemPhysChem* **2005**, *6*, 1221.
- (8) Wiley, B. J.; Chen, Y.; McLellan, J.; Xiong, Y.; Li, Z.-Y.; Ginger, D.; Xia, Y. *Nano Lett.* **2007**, *7*, 1032.
- (9) Lee, S. J.; Morrill, A. R.; Moskovits, M. *J. Am. Chem. Soc.* **2006**, *128*, 2200.
- (10) Zeman, E. J.; Schatz, G. C. *J. Phys. Chem.* **1987**, *91*, 634.
- (11) Yang, W.-H.; Schatz, G. C.; Van Duyne, R. P. *J. Chem. Phys.* **1995**, *103*, 869.
- (12) Jeong, D. H.; Zhang, Y. X.; Moskovits, M. *J. Phys. Chem. B* **2004**, *108*, 12724.
- (13) Byun, K. M.; Kim, S. J.; Kim, D. *Appl. Opt.* **2006**, *45*, 3382.
- (14) Byun, K. M.; Yoon, S. J.; Kim, D.; Kim, S. J. *Opt. Lett.* **2007**, *32*, 1902.
- (15) Yu, C.; Irudayaraj, J. *Biophys. J.* **2007**, *93*, 3684.
- (16) Marinakos, S. M.; Chen, S.; Chilkoti, A. *Anal. Chem.* **2007**, *79*, 5278.
- (17) Kong, D. S.; Varsanik, J. S.; Griffith, S.; Jacobson, J. M. *J. Vac. Sci. Technol. B* **2004**, *22*, 2987.
- (18) Plaza, J. L.; Chen, Y.; Jacke, S.; Palmer, R. E. *Langmuir* **2005**, *21*, 1556.

- (19) Claus, P.; Hofmeister, H. *J. Phys. Chem. B* **1999**, *103*, 2766.
- (20) Lopez-Salido, I.; Lim, D. C.; Kim, Y. D. *Surf. Sci.* **2005**, *598*, 96.
- (21) Mallick, K.; Witcomb, M.; Scurrell, M. *Mater. Chem. Phys.* **2006**, *97*, 283.
- (22) Tsujino, K.; Matsumura, M. *Adv. Mater.* **2005**, *17*, 1045.
- (23) Wei, Q.; Li, B.; Li, C.; Wang, J.; Wang, W.; Yang, X. *J. Mater. Chem.* **2006**, *16*, 3606.
- (24) Zidki, T.; Cohen, H.; Meyerstein, D. *Phys. Chem. Chem. Phys.* **2006**, *8*, 3552.
- (25) Sun, X.; Li, Y. *Adv. Mater.* **2005**, *17*, 2626.
- (26) Jana, N. R.; Gearheart, L.; Murphy, C. J. *Chem. Commun.* **2001**, 617.
- (27) Sun, Y.; Xia, Y. *Adv. Mater.* **2002**, *14*, 833.
- (28) Caswell, K. K.; Bender, C. M.; Murphy, C. J. *Nano Lett.* **2003**, *3*, 667.
- (29) Hu, J.-Q.; Chen, Q.; Xie, Z.-X.; Han, G.-B.; Wang, R.-H.; Ren, B.; Zhang, Y.; Yang, Z.-L.; Tian, Z.-Q. *Adv. Funct. Mater.* **2004**, *14*, 183.
- (30) Maddani, T.; Kumar, A.; D'Arcy-Gall, J.; Ganesan, P. G.; Vijayamohan, K.; Ramanath, G. *Chem. Commun.* **2005**, 1435.
- (31) Wang, Z.; Liu, J.; Chen, X.; Wan, J.; Qian, Y. *Chem.—Eur. J.* **2005**, *11*, 160.
- (32) Halder, A.; Ravishankar, N. *Adv. Mater.* **2007**, *19*, 1854.
- (33) Zhao, X.-G.; Shi, J.-L.; Hu, B.; Zhang, L.-X.; Hua, Z.-L. *Mater. Lett.* **2004**, *58*, 2152.
- (34) Asefa, T.; Lennox, R. B. *Chem. Mater.* **2005**, *17*, 2481.
- (35) Shimizu, T.; Masuda, M.; Minamikawa, H. *Chem. Rev.* **2005**, *105*, 1401.
- (36) Tsung, C.-K.; Hong, W.; Shi, Q.; Kou, X.; Yeung, M. H.; Wang, J.; Stucky, G. D. *Adv. Funct. Mater.* **2006**, *16*, 2225.
- (37) Wang, H.-H.; Liu, C.-Y.; Wu, S.-B.; Liu, N.-W.; Peng, C.-Y.; Chan, T.-H.; Hsu, C.-F.; Wang, J.-K.; Wang, Y.-L. *Adv. Mater.* **2006**, *18*, 491.
- (38) Mohanty, P.; Yoon, I.; Kang, T.; Seo, K.; Varadwaj, K. S. K.; Choi, W.; Park, Q. H.; Ahn, J. P.; Suh, Y. D.; Ihee, H.; Kim, B. *J. Am. Chem. Soc.* **2007**, *129*, 9576.
- (39) Yang, B.; Kamiya, S.; Yoshida, K.; Shimizu, T. *Chem. Commun.* **2004**, 500.
- (40) Wang, H.; Qi, L. *Adv. Funct. Mater.* **2008**, *18*, 1249.

to tune the final Ag(I) and Ag(0) nanostructure size, in terms of both length and width. Moreover, none of these methods have been shown to be suitable for a large-scale production of nanocomposites.

We present here a simple, reproducible, high-yield, large-scale (>100 mg), and inexpensive route to produce silver nanowire arrays from AgNO<sub>3</sub> and poly(styrene-*alt*-maleic anhydride, SMA). SMA was recently shown to self-assemble and form nanotubes in aqueous media.<sup>42,43</sup> The technique described here takes advantage of this structural property to guide silver cyanide (AgCN) growth into a very high aspect ratio (500 to 10000) nanowires (5–200 nm wide, >50 μm long). Subsequent chemical reduction of the composite deposited on a nylon filter with sodium borohydride (NaBH<sub>4</sub>) leads to the formation of a porous conductive metallic silver nanowire network. Silver cyanide is a common silver precursor, often used in silver electroplating.<sup>44–47</sup> Long AgCN nanowires have not however been reported, opening a range of possibilities for AgCN-based nanocomposites. The synthesis of a new AgCN–SMA composite with interesting and tunable geometry, shapes, and structures is presented.

## 2. Experimental Section

**2.1. Materials.** Poly(styrene-*alt*-maleic anhydride) was purchased from SP<sup>2</sup> Scientific Polymer Source (1.6 and 50 kDa). Silver nitrate (>99%), silver cyanide, sodium borohydride, and cyanoborohydride were purchased from Aldrich, and potassium cyanide was purchased from Anachemia. All were used as-received.

**2.2. Instruments.** The pH was measured using an Accumet Basic AB15 (Fisher Scientific). Transmission electron microscopy (TEM) measurements were performed on a JEOL JEM-2000FX 200 kV, operated at 80 kV. High-resolution TEM was performed on a JEOL JEM-2011 200 kV TEM. Scanning electron microscopy (SEM) measurements were performed using an Hitachi S-4700 FEG-SEM operated between 5 and 15 kV. Energy-dispersive X-ray spectroscopy (EDS) measurements were performed on the same FEG-SEM, using Oxford INCA EDS hardware. Typical conditions during the spectra acquisitions were as follows: size of the area analyzed, 5 μm; electron beam energy, 10 kV; acquisition time, 90 s. Size analysis measurements were performed using SigmaScan Pro (version 4). Two-point conductivity measurements were performed using a digital multimeter (Extech Multimaster 570 True rms). Powder X-ray diffraction was performed using a Siemens D-5000 with a Globel mirror.

**2.3. SMA Nanotube Preparation.** The SMA polymer nanotube preparation method (in deionized water) was the same for the two different  $M_w$  samples. An SMA solution of 0.1 wt % was prepared in deionized water. The maleic anhydride groups of SMA were hydrolyzed using an excess of NaOH, to obtain a pH beyond the second pK<sub>a</sub> (pK<sub>a2</sub> = 10.3).<sup>48</sup> Three mole equivalents of NaOH (by weight, relative to SMA monomer) was added (SMA monomer =

(styrene–maleic anhydride)). The base was dissolved in deionized water, and the polymer was added to the solution and then stirred until it dissolved (overnight). A 50% degree of protonation was achieved by dialyzing the basic solution against 2 L of deionized water, using 1000 Da cutoff membranes (SpectraPore). The water was changed 2 times per day and the pH inside the dialysis bag recorded after every water change, over 2–3 days. When the solution inside the dialysis bag reached pH 7.5–8, the dialysis was stopped and the solution stored in polyethylene bottles.

**2.4. AgCN–SMA Composite with NaBH<sub>3</sub>CN.** The concentration (wt %) of experimental solutions was determined using the UV–vis absorbance at 258 nm, and an absorbance–concentration calibration curve was generated.

AgCN–SMA nanowires were prepared by dissolving 2 mol equiv of AgNO<sub>3</sub> (relative to SMA monomer) in 5 mL of deionized water and then adding the silver salt solution dropwise to the SMA nanotube solution. SMA concentrations used were on the order of  $2–5 \times 10^{-3}$  g/mL. Four mole equivalents of NaBH<sub>3</sub>CN was dissolved in 5 mL of water and added dropwise to the solution over a period of 2 min while stirring vigorously. The solution turned opaque dark brown upon addition of the reducing agent. Stirring was then reduced to 40 rpm. Over 2 days, bundles of nanowires precipitated from solution as a white fibrous material. The final solution was pale orange and transparent with white fibrous precipitates. A lower aggregation number of SMA was observed when the reduction was carried out while sonicating the sample for the duration of the experiment. The precipitate was cleaned by successive centrifugation in deionized water at 6000 rpm, giving a highly fibrous white material.

**2.5. AgCN–SMA Composite with KCN.** Two mole equivalents of AgNO<sub>3</sub> (relative to SMA monomer) was dissolved in 5 mL of deionized water. The silver salt was added dropwise to the SMA nanotube solution. SMA concentrations were on the order of  $2–5 \times 10^{-3}$  g/mL. Four mole equivalents of KCN was dissolved in 5 mL of water and added dropwise to the solution over a period of 2 min while stirring. An insoluble white precipitate appeared after a few minutes.

**2.6. Conductive Ag Nanowire Array with a Grid Pattern.** A conductive grid was produced by filtering 5 mL of unsonicated AgCN–SMA, prepared from 50 kDa SMA through a plain 47 mm Nylon filter (Advantec MFS Inc., 0.45 μm), using a peristaltic pump. The sample was thoroughly washed with deionized water. A second nylon filter was deposited over the filtered nanotube film and pressed between porous paper sheets under 50 psi pressure to remove excess water and form a flat film. The flattened filters were reintroduced onto the grid pattern filter support. 132 mM NaBH<sub>4</sub> was dissolved in 20 mL of water and the solution was passed through the filters using the peristaltic pump. The final sample was washed with deionized water. Only the support areas of the grid retained the Ag nanowires, producing a grid pattern. The filtration step on the nylon membrane was also performed on a glass frit for the investigation of the reduction mechanism using 1.6 kDa AgCN–SMA network.

## 3. Results and Discussion

**3.1. SMA Polymer Nanotube Template.** Molecular modeling of the association properties of 50% protonated hydrolyzed SMA has shown that the polymer molecules align themselves sideways to form linear association complexes.<sup>42,43</sup> Multiple associations form a minimum energy closed tubular structure involving eight SMA polymers (Scheme 1). This nanotube structure grows via the addition of further polymers along the edges of the tube. Additional  $\pi$ -stacking at the

(41) Viau, G.; Piquemal, J.-Y.; Esparrica, M.; Ung, D.; Chakroune, N.; Warmont, F.; Fievet, F. *Chem. Commun.* **2003**, 2216.

(42) Malardier-Jugroot, C.; van de Ven, T. G. M.; Cosgrove, T.; Richardson, R. M.; Whitehead, M. A. *Langmuir* **2005**, *21*, 10179.

(43) Malardier-Jugroot, C.; van de Ven, T. G. M.; Whitehead, M. A. *Mol. Simul.* **2005**, *31*, 173.

(44) Ashiru, O. A.; Farr, J. P. G. *J. Electrochem. Soc.* **1995**, *142*, 3729.

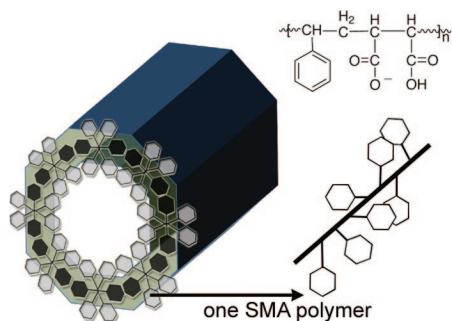
(45) Krishnan, R. M.; Sriveeraraghavan, S.; Deenadayalan, M.; Jayakrishnan, S.; Sekar, R.; Jayachandran, P. *Bull. Electrochem.* **2000**, *16*, 136.

(46) Pan, L. C. *Trans. Electrochem. Soc.* **1931**, *59*, 5.

(47) Sanchez, H.; Chainet, E.; Nguyen, B.; Ozil, P.; Meas, Y. *J. Electrochem. Soc.* **1996**, *143*, 2799.

(48) Garret, E. R.; Guile, R. L. *J. Am. Chem. Soc.* **1951**, *73*, 4533.

**Scheme 1. Schematic of the Polymer Nanotube Formed by a Process Where Eight SMA Polymer Chains Self-associate Sideways by  $\pi$ -Stacking of the Styrene Rings<sup>a</sup>**



<sup>a</sup> Cross-sectional view of the tube is shown and the polymer chains lie along the sidewalls of the nanotube.

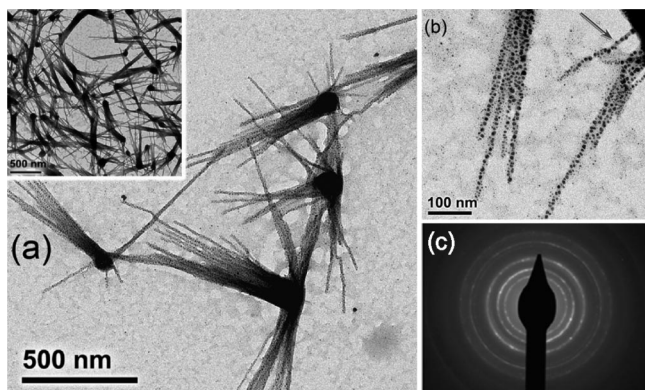


**Figure 1.** (a) TEM images of AgCN-SMA (1.6 kDa) nanowires formed using  $\text{NaBH}_3\text{CN}$ . The AgCN-SMA nanowires observed are joined in bundles, stacked linearly. Inset: low-magnification TEM image showing many clusters of stacked nanowires. (b) Enlarged view of the composite nanowires (1.6 kDa). The arrow shows the location of an individual AgCN-SMA nanowire composite measuring between 5 and 10 nm in diameter. (c) Electron diffraction pattern of AgCN-SMA (1.6 kDa) nanowire bundles showing the non fcc structure of the resulting nanocomposite.

periphery of the nanotubes drives sideways aggregation, yielding SMA nanotube bundles. Molecular modeling predicts that the lowest energy SMA nanotubes have an outer diameter of about 5 nm and an inner diameter of about 2 nm.<sup>43</sup>

**3.2. AgCN-SMA Nanowire Fabrication.** SMA (1.6 and 50 kDa) nanotubes prepared by dialysis were used to template the growth of silver cyanide via the reduction of silver nitrate with sodium cyanoborohydride ( $\text{NaBH}_3\text{CN}$ ). Over the 2 day period reaction, a fibrous composite results. The nanowires precipitate in bundles with a range of aggregation numbers and lengths, dependent on the molecular weight of the SMA polymer and on the use of sonication.

The fiber nanowire bundles are polydisperse, but are made up of monodisperse building blocks (individual nanotubes). The diameter of these individual nanowires is similar for both the 1.6 kDa and the 50 kDa samples ( $5.2 \pm 0.9$  nm) and is close to that of the theoretical outer diameter for a single SMA nanotube. The aggregation number is also similar in both cases. Figures 1 and 2 are TEM images

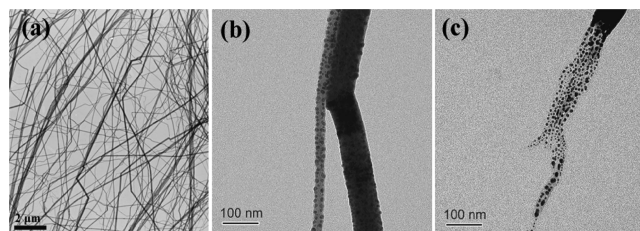


**Figure 2.** TEM images. (a) and (b) AgCN-SMA (50 kDa) nanowires with AgCN formed along and within the nanotubes. The wires are actually composed of nanotube clusters, each of about 5 nm diameter, stacked together to form larger wires. These larger wires have polydisperse diameters. (c) An AgCN-SMA (50 kDa) nanowire bundle, measuring ca. 75 nm in diameter, shows the individual nanotubes that build up the larger bundle of nanowires.

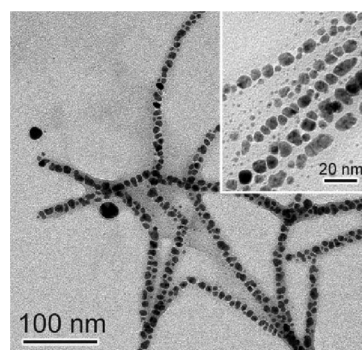


**Figure 3.** TEM image of AgCN-SMA nanowires formed using 1.6 kDa SMA while sonicating the sample. Reduction with  $\text{NaBH}_3\text{CN}$  was performed during sonication of the solution. The average diameter of the wires corresponds to bundles of less than five nanotubes. Inset: High-resolution TEM image showing single nanotubes and bundles of two nanotubes.

showing the structure for both SMA precursors (1.6 and 50 kDa) of these aggregates, composed of multiple individual nanowires.

**3.2.1. AgCN-SMA (1.6 kDa) Nanowires.** Using SMA (1.6 kDa) results in bundle formation of 5–20 AgCN-SMA nanowires, joined together at one end. TEM images (Figure 1) of the structures clearly show the formation of bundles. Nanowire length is typically between 500 nm and 1  $\mu\text{m}$ .

**3.2.2. AgCN-SMA (50 kDa) Nanowires.** When 50 kDa SMA nanotubes are used to template the growth of AgCN, one observes nanowires that are 1–2 orders in magnitude longer than those with the 1.6 kDa SMA (Figure 2). These can reach lengths greater than 50  $\mu\text{m}$  (SEM image, Supporting Information). They appear as large fibers as they are formed from tightly arranged bundles of 5–20 nanowires.

**3.2.3. Individual Nanowire Fabrication Using Sonication.** The extent of nanotube aggregation is decreased by sonication of the sample during the reduction process. The tertiary structure of SMA self-assembly into bundles of nanotubes is weaker than the secondary structure of self-assembly into nanotubes. Sonication was carried out prior to and during the addition and reduction of  $\text{AgNO}_3$ . This allows for the preparation of isolated AgCN-SMA nanowires. These are observed as bundles of less than five nanowires. High-resolution TEM scans (inset in Figure 3) shows the microstructure of the nanowires. Comparison of Figures 1 (not

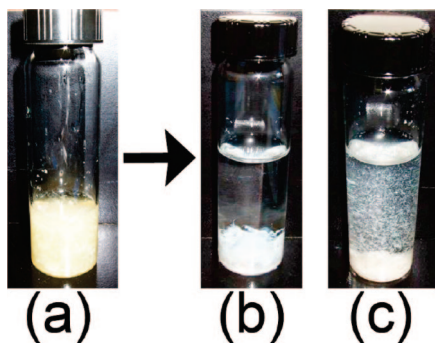


**Figure 4.** AgCN-SMA nanocomposites in glass vials. AgCN-SMA (50 kDa) before (a) and after washing with deionized water (b). Washed AgCN-SMA (1.6 kDa) (c). The yellowish color of the Ag NP solution, seen in (a), disappears upon washing, giving a white precipitate with both SMA precursors (50 and 1.6 kDa) as seen in (b) and (c).

sonicated) and 3 (sonicated) clearly shows that stacking of individual nanotubes can be limited using sonication.

**3.2.4. AgCN-SMA Nanowire Formation Mechanism.** The mechanism leading to the formation of these nanocomposites can be described by a two-step process. First, silver ions are reduced by  $\text{NaBH}_3\text{CN}$  to form silver nanoparticles (Ag NP). Until the reducing power of  $\text{NaBH}_3\text{CN}$  is depleted, the solution has the characteristic orange color of Ag NP in water,<sup>4-6,49</sup> (UV-vis spectra, Supporting Information). Carboxylic acids are known to be good stabilizing agents for Ag NP,<sup>50</sup> suggesting that SMA may serve as a protecting ligand in this regard.  $\text{CN}^-$  could also stabilize the Ag NP, but carrying the reaction without SMA precipitates silver as Ag(0). This step is rapid and takes place in solution as in typical water-phase nanoparticle syntheses.

The second step is slow and involves the growth of silver cyanide within the polymer nanotubes, forming AgCN-SMA nanowires that precipitate as white fibers. Over the 2 day formation of the precipitate,  $\text{CN}^-$  is released, scavenging silver from the NP and reacting with free  $\text{Ag}^+$  ions to form AgCN with the SMA nanotubes. The AgCN nanowire structure becomes insoluble and precipitates out of solution as a white yellowish fibrous aggregate. The yellowish tint disappears upon washing and likely arises from adsorbed silver NP within the nanowire network (Figure 4). It is important to note that the dialysis step, which brings the pH down from 12 to around 8 over a period of 48 h, is crucial for obtaining these nanowire structures. Changing the pH rapidly by addition of acid or base does not produce uniform structures as observed in Figures 1, 2, and 3.

When the quantity of  $\text{NaBH}_3\text{CN}$  is decreased by a factor of 20 or when  $\text{NaBH}_4$  is used as the primary reducing agent, no precipitate is formed. Instead, a clear orange solution involving noninteracting silver  $\text{NP}^{4-6,49}$  is observed (TEM, Figure 5). These experiments show that  $\text{NaBH}_3\text{CN}$  is essential for making these nanowires.

$\text{NaBH}_3\text{CN}$ , often used in organic synthesis for reduction of amines,<sup>51</sup> acts here as both the reducing agent and the

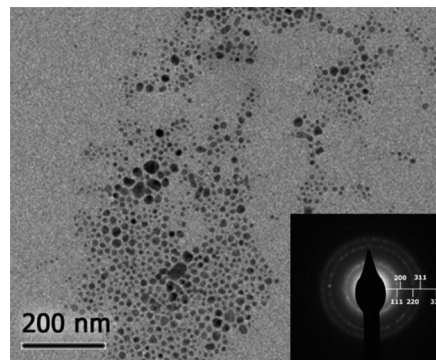


**Figure 5.** TEM image of the NP formed when the quantity of  $\text{NaBH}_3\text{CN}$  is decreased by a factor of 20 or when  $\text{NaBH}_4$  is used as the reducing agent. Only nanoparticles are observed and no nanowires are formed. Inset: related electron diffraction pattern showing the fcc structure of the Ag NP. The rings observed are due to the numerous Ag NP with different orientations on the TEM grid. The  $\pi$ -stacking, which maintains the nanotube structure, is disrupted when the sample is dried or exposed to an electron beam. The SMA nanotubes are not apparent in the TEM.

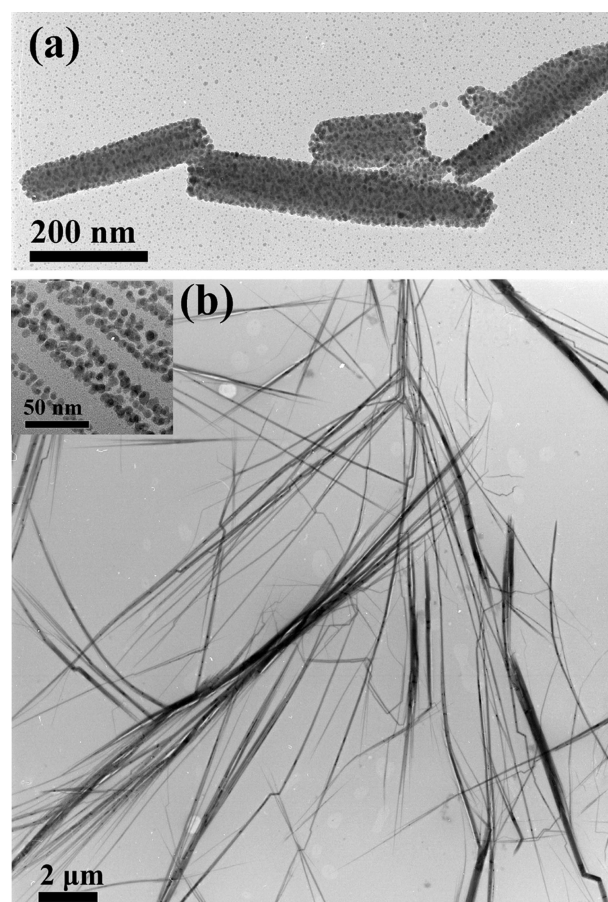


**Figure 6.** TEM images. (a)  $\text{AgNO}_3$  dissolved in deionized water with KCN; short linear nanowires are obtained, showing that AgCN grows linearly. However, the nanostructures formed are much shorter than those in the presence of SMA. (b) KCN instead of the reducing agent was added to the  $\text{AgNO}_3$ -SMA (50 kDa) solution. Similar AgCN-SMA nanowires were obtained without the use of the reducing agent  $\text{NaBH}_3\text{CN}$ . Inset: TEM image of a sample prepared with 1.6 kDa SMA.

cyanide source. Because  $\text{BH}_3\text{CN}^-$  hydrolysis is extremely slow in neutral aqueous media,<sup>52</sup> the reduction of  $\text{Ag}^+$  by

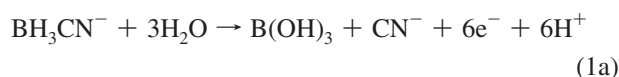
(49) Evanoff, D. D.; Chumanov, G. *ChemPhysChem* **2005**, *6*, 1221.

(50) Lee, P. C.; Meisel, D. *J. Phys. Chem.* **1982**, *86*, 3391.

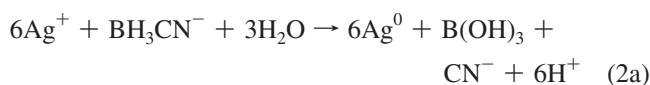
(51) Borch, R. F.; Bernstei, M. D.; Durst, H. D. *J. Am. Chem. Soc.* **1971**, *93*, 2897.

(52) Berschied, J. R.; Purcell, K. F. *Inorg. Chem.* **1970**, *9*, 624.

NaBH<sub>3</sub>CN provides the cyanide (eq 1a) required for the silver cyanide formation.<sup>52,53</sup> Indeed, the oxidation half-reaction of BH<sub>3</sub>CN<sup>-</sup> in aqueous media is



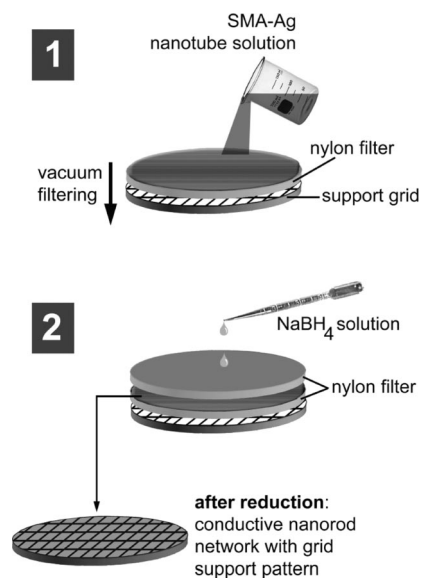
and the overall reduction of silver(I) by NaBH<sub>3</sub>CN is then given by



Cyanide reacts with Ag<sup>+</sup> and Ag(0), forming complex ions such as Ag(CN)<sub>2</sub><sup>-</sup>. A silver cyanide precipitates from an aqueous medium.<sup>54–57</sup> Ag(0) dissolution in an O<sub>2</sub> containing CN<sup>-</sup> solution is a four-electron oxidation process, involving the reduction of O<sub>2</sub> adsorbed on the metal surface (Supporting Information).<sup>57</sup> Reduction of silver nitrate with NaBH<sub>3</sub>CN in the presence of SMA in an argon atmosphere did not form any wires after 4 days, clearly showing that O<sub>2</sub> is essential for making the AgCN–SMA nanowires. This is in agreement with the proposed mechanism involving the oxidation of the Ag NP by O<sub>2</sub> in the presence of CN<sup>-</sup>, to form silver cyanide.

Like the metal cyanides AuCN and CuCN, AgCN forms infinite –M–(CN)– 1D chains, packed through argentophilic interactions into a trigonal structure.<sup>55,58,59</sup> This ability to form one-dimensional chains has already been used to create several well-defined molecular structures such as a fivefold helix and a fishnet-shaped framework structure.<sup>60</sup> The presence of silver cyanide is verified by energy-dispersive X-ray spectroscopy (Supporting Information) and IR spectroscopy (Supporting Information), the latter with the appearance of a sharp peak at 2165 cm<sup>-1</sup>, characteristic of the CN bond in AgCN.<sup>55</sup> Selected area electron diffraction pattern (SAED) establishes that the dark nanoaggregates visualized along and within the wires are not Ag(0) (Figure 1c). This is further supported by the absence of the localized SPR peak around 400 nm, characteristic of Ag NP (UV–vis spectra, Supporting Information and Figure 4). X-ray powder diffraction (XRD) reveals that the as-synthesized AgCN–SMA composites are exclusively composed of AgCN (Supporting Information). The structure of AgCN is still under debate because of defaults within the linear Ag–CN chains,<sup>55,58,59</sup> and the exact determination of AgCN crystallographic structure goes beyond the scope of this work. Peak indexation was performed using JCPDS data (23-1404) assuming a trigonal crystal. The high background of the AgCN XRD pattern is due to its poor crystallinity.<sup>55</sup> XRD analysis of AgCN and AgCN–SMA is strong evidence for formation

## Scheme 2. Schematic Representation of the Process Used To Produce Conductive Arrays of Ag(0) Nanowires from AgCN–SMA Nanowires<sup>a</sup>



<sup>a</sup> (1) Deposition of precipitated bundles of AgCN–SMA (50 kDa) nanowires. (2) Reduction of AgCN–SMA using a NaBH<sub>4</sub> solution. The nanowire network and most of the polymer are removed. Conductivity is assessed using the two-point probe method.

of AgCN along the SMA nanotubes and the absence of metallic Ag NP within the nanowires formed during the second, slow reaction step.

Nanowire formation was further investigated by reacting silver nitrate with KCN.<sup>55</sup> This was performed in the presence and absence of the SMA polymer template in solution. In the presence of SMA, similar structures are obtained when using NaBH<sub>3</sub>CN (Figure 6). Without the SMA template, a white precipitate of silver cyanide is formed. TEM investigation shows that shorter AgCN nanowires (up to 500 nm in length) are likely to be formed. However, these linear structures are present in a small quantity.

Reduction of AgNO<sub>3</sub> with NaBH<sub>3</sub>CN using citrate as the stabilizer produces nanoparticles only and no nanowires. This confirms that nanowire formation requires the presence of the SMA template.

Thermal gravimetric analysis was performed on AgCN–SMA (50 kDa) nanowires which had been centrifuged three times in deionized water and freeze-dried (Supporting Information). A material with 78.4% noncombustible inorganic content, corresponding to Ag content results, consistent with the material being AgCN (80.5% by weight Ag). A recovered yield of 63% (relative to Ag) is observed. The reaction can be performed on the >100 mg scale (i.e. 200 mg of AgCN–SMA nanowires are readily synthesized in a single batch). The yield increases using the 50 kDa SMA polymer. The yield using AgNO<sub>3</sub> and KCN (24%) is less than that using NaBH<sub>3</sub>CN. This composite has been stable over a period of 1 year when stored at room temperature in deionized water, protected from the light.

**3.3. Conductivity of the Metallic Nanowire Array Obtained via Chemical Reduction.** The AgCN–SMA nanowire network is reduced to metallic silver with NaBH<sub>4</sub>. A

(53) Kreevoy, M. M.; Hutchins, J. E. *J. Am. Chem. Soc.* **1969**, *91*, 4329.

(54) Azzam, A. M.; Shimi, I. A. W. *Z. Anorg. Allg. Chem.* **1963**, *321*, 284.

(55) Bowmaker, G. A.; Kennedy, B. J.; Reid, J. C. *Inorg. Chem.* **1998**, *37*, 3968.

(56) Guebeli, A. O.; Cote, P. A. *Can. J. Chem.* **1972**, *50*, 1144.

(57) Hiskey, J. B.; Sanchez, V. M. *J. Appl. Electrochem.* **1990**, *20*, 479.

(58) Hibble, S. J.; Cheyne, S. M.; Hannon, A. C.; Eversfield, S. G. *Inorg. Chem.* **2002**, *41*, 1042.

(59) Bryce, D. L.; Wasylishen, R. E. *Inorg. Chem.* **2002**, *41*, 4131.

(60) Urban, V.; Pretsch, T.; Hartl, H. *Angew. Chem., Int. Ed.* **2005**, *44*, 2794.

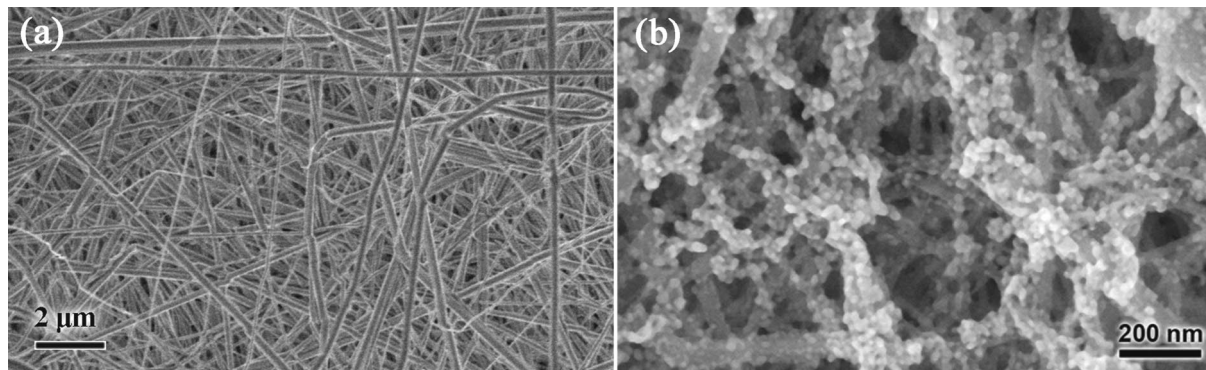


**Figure 7.** (a) SEM image of AgCN–SMA (50 kDa) nanowire bundles deposited on a nylon 0.45  $\mu\text{m}$  filter. (b) SEM image of AgCN–SMA (1.6 kDa) nanowire bundles deposited on a nylon 0.45  $\mu\text{m}$  filter treated with a small quantity of a 2.6 mM  $\text{NaBH}_4$  solution. This demonstrates the intermediate reduction of the AgCN–SMA composite to Ag(0).

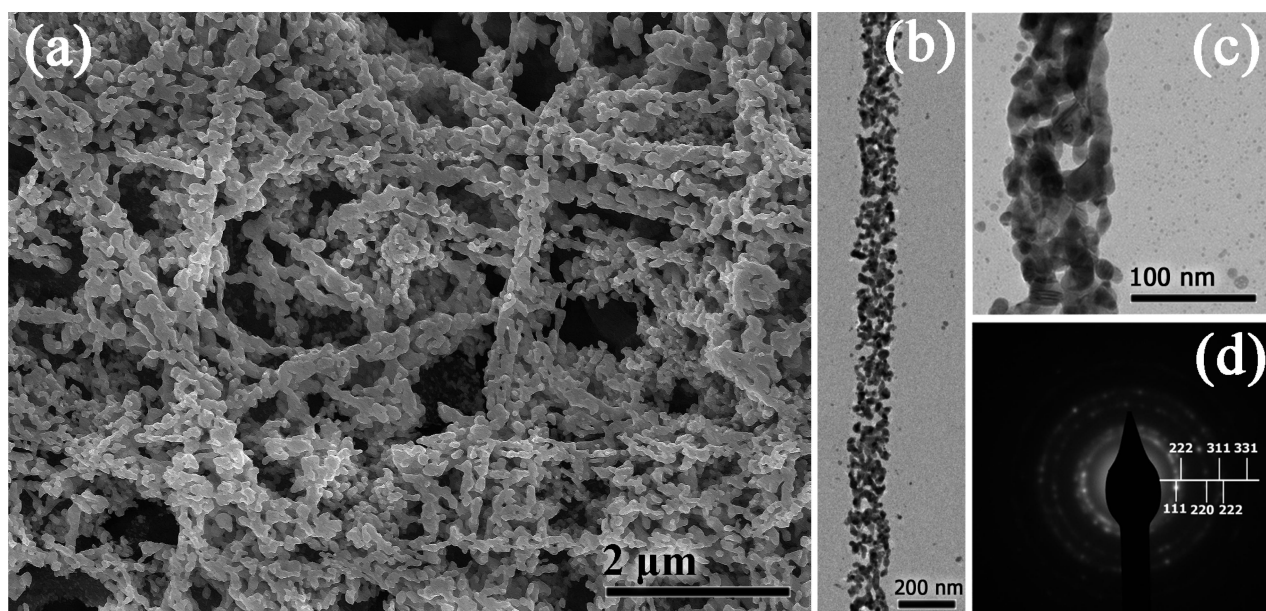


**Figure 8.** (a) SEM image of the interconnected Ag nanowire conductive network obtained from AgCN–SMA (50 kDa) bundles treated with  $\text{NaBH}_4$  on the nylon filter. (b) TEM image of an individual AgCN–SMA (50 kDa) nanowire bundle reduced on a carbon TEM grid between two nylon filters. (c) Zoom of the resulting continuous Ag metallic nanowire formed from aggregated Ag NP. (d) Electron diffraction pattern of the nanowire seen in (b) and (c), clearly showing its metallic polycrystalline fcc structure.

dedicated set-up (periodic grid, nylon filter, and peristaltic pump) was used to pattern the resulting conductive network at the millimeter scale level (Scheme 2). The initial AgCN–SMA network (Figure 7a) is quickly transformed into a metallic silver nanowire network via  $\text{NaBH}_4$  reduction (Figure 8). The intermediate state of the composite during the reduction step (Figure 7b) yields the white dots corresponding to the regions where AgCN has been reduced and begins to aggregate along the wires. The nanostructures obtained have similar dimensions to the initial ones and the nature of the network is preserved to a certain extent. TEM, SAED (Figure 8), and powder XRD (Supporting Information) of the resulting Ag(0) nanowires clearly show that they are exclusively composed of aggregated Ag(0) NP. They are polycrystalline and are made of pure metallic silver as per their fcc structure. XRD pattern of the reduced nanowires was indexed using JCPDS data (4-783) and correspond to the fcc structure of silver.

Two-point probe electrical measurements performed at multiple locations on the dried sample (i.e., Figure 8) establishes that the resistance is 100–300  $\Omega$  (distances from

1 to 10 mm) on the remaining pattern. A huge resistance is measured outside the array.<sup>61</sup> We conclude that the AgCN–SMA nanowires indeed can be transformed into Ag(0) nanowires.

#### 4. Concluding Remarks

We have demonstrated that SMA nanotubes can be used as templates to form highly stable networks of AgCN–SMA and Ag nanowires on a large scale. In contrast to previous work using self-assembled Ag(I) precursors,<sup>40,41</sup> the length and width of the AgCN–SMA nanocomposites can be tuned by modification of the  $M_w$  of the polymer and by sonication to prevent stacking between the SMA nanotubes. AgCN is believed to form along the length of the nanotubes and its

(61) Those values include the contact resistance: as a reference, the resistance measurements on a copper wire (1 mm wide and 1 cm long) gave values of 0.2  $\Omega$ , equivalent to a resistivity of  $6.3 \times 10^{-5} \Omega\text{-m}$ , which is 3 orders of magnitude higher than the literature value ( $\rho_{\text{Cu}} = 1.712 \times 10^{-8} \Omega\text{-m}$  at 298 K). The contact resistance involved in the nanowire resistance measurement is thus at least 0.2  $\Omega$ .

reduction to metallic silver may be supported by the polymer scaffold of the SMA template.

A fast chemical reduction of the AgCN–SMA composite into a conductive and porous material has been demonstrated using a soft chemical process, allowing the use of an organic substrate such as nylon to deposit this network. The high stability of these composites (up to 1 year in ambient conditions) and their fast transformation (within few minutes) into a conductive network is an addition to the methods which provide simple and accessible nanomaterial syntheses. A continuous conductive network has been produced. This template system has the potential of being used to produce single conductive wires and will be the focus of further

research. Both the silver cyanide and the silver structures are soluble in nitric acid, allowing them to be used as reverse templates.

**Acknowledgment.** The authors thank the Natural Sciences and Engineering Research Council of Canada and the Center for Self Assembled Chemical Structures (FQRNT) for their financial support. David Liu is thanked for obtaining the electron diffraction pattern.

**Supporting Information Available:** Additional figures. This material is available free of charge via the Internet at <http://pubs.acs.org>.

CM802481V